UDC 621.74 + 669.018
https://doi.org/10.17073/0021-3438-2023-4-70-86

Research article
Научная статья

Liquid matrix SHS manufacturing and heat treatment of Al–Mg composites reinforced with fine titanium carbide

A.R. Luts, Yu.V. Sherina, A.P. Amosov, A.D. Kachura

Samara State Technical University
244 Molodogvardeyskaya Str., Samara 443100, Russia,

✉ Alexander P. Amosov (egundor@yandex.ru)

Abstract: Aluminum matrix composites reinforced with ultra-fine refractory titanium carbide feature a unique combination of properties. They are promising structural materials. Self-propagating high-temperature synthesis (SHS) is an affordable and energy-saving composite-making process. It involves the exothermic reaction between titanium and carbon (or their compounds) directly in the melt. We studied the properties of SHS composites based on the AMg2 and AMg6 commercially available alloys reinforced with 10 wt.%TiC. We investigated the macro- and microstructure of the samples with XRD and EDS analysis. It was found that the β-phase is separated from α-solid solution of aluminum as early as the air cooling stage. We conducted experiments aimed at studying the effects of additional heating on the sample structure and properties and found the optimal temperature and time values. We also proposed a phenomenological model of the structural transformation sequence. We compared the physical, mechanical, and manufacturing properties and corrosion resistance of the original cold-hardened AMg2N and AMg6N alloys and the composites before and after heat treatment. It was found that additional heating reduces porosity and maintains electrical conductivity. It was also found that the compressive strength and relative strain of the composite based on the AMg2 alloy change insignificantly, while for the AMg6-based composite the reduction is more significant. Heat treatment increases the composite hardness while maintaining sufficient plastic deformation. It is confirmed by the measured values of the relative strain and the reduction ratio close to that of the original matrix alloys. It was also found that the composites retain high resistance to carbon dioxide and hydrogen sulfide corrosion.

Keywords: aluminum matrix composite (AMCs), aluminum, melt, titanium carbide, self-propagating high-temperature synthesis (SHS).

For citation: Luts A.R., Sherina Yu.V., Amosov A.P., Kachura A.D. Liquid matrix SHS manufacturing and heat treatment of Al–Mg composites reinforced with fine titanium carbide. *Izvestiya. Non-Ferrous Metallurgy.* 2023;29(4):70–86.
https://doi.org/10.17073/0021-3438-2023-4-70-86

Жидкофазное получение методом СВС и термическая обработка композитов на основе алюминиево-магниевых сплавов, упрочненных высокодисперсной фазой карбида титана

А.Р. Луц, Ю.В. Шерина, А.П. Амосов, А.Д. Качура

Самарский государственный технический университет
443100, Россия, г. Самара, ул. Молодогвардейская, 244

✉ Александр Петрович Амосов (egundor@yandex.ru)

Аннотация: Алюмоматричные композиционные материалы, дисперсно-упрочненные тугоплавкой фазой карбида титана, характеризуются уникальным сочетанием свойств и относятся к группе перспективных конструкционных материалов. Одним из наи-

более доступных и энергосберегающих методов их получения является самораспространяющийся высокотемпературный синтез (СВС), основанный на экзотермическом взаимодействии титана и углерода (или их соединений) непосредственно в расплаве. В работе приводятся результаты СВС композиционных материалов на основе промышленных сплавов АМг2Н и АМг6Н, упрочненных 10 мас.%TiC. Исследованы макро- и микроструктура полученных образцов, проведены микрорентгеноспектральный и рентгенофазовый анализы. Установлено, что уже в процессе охлаждения на воздухе после синтеза происходит выделение β-фазы из α-твердого раствора алюминия. Проведены эксперименты по изучению влияния дополнительного нагрева на структуру и свойства образцов, определены оптимальные температурно-временные параметры, предложена феноменологическая модель последовательности структурных превращений. Выполнен сравнительный анализ физических, механических, технологических свойств и коррозионной стойкости исходных сплавов АМг2Н и АМг6Н в нагартованном состоянии и композиционных материалов на их основе до и после термической обработки. Установлено, что проведение дополнительного нагрева способствует снижению пористости и сохранению уровня электропроводности относительно этих показателей для литых композитов. Выявлено, что прочность на сжатие и относительная деформация для композита на основе сплава АМг2 изменяются незначительно, тогда как для материала на основе АМг6 их падение более существенно. При этом термическая обработка позволяет повысить твердость материалов, сохранив достаточную способность композитов к пластической деформации, что подтверждается значениями степени деформации и коэффициента уковки, близкими к уровню матричных сплавов. Также установлено, что синтезированные композиционные материалы сохраняют высокий уровень устойчивости к углекислотной и сероводородной коррозии.

Ключевые слова: алюмоматричный композиционный материал (АМКМ), алюминий, расплав, карбид титана, самораспространяющийся высокотемпературный синтез (СВС).

Для цитирования: Луц А.Р., Шерина Ю.В., Амосов А.П., Качура А.Д. Жидкофазное получение методом СВС и термическая обработка композитов на основе алюминиево-магниевых сплавов, упрочненных высокодисперсной фазой карбида титана. *Известия вузов. Цветная металлургия*. 2023;29(4):70–86. https://doi.org/10.17073/0021-3438-2023-4-70-86

Introduction

Aluminum matrix composites (AMCs) reinforced with fine refractory titanium carbide (from hundredths of a percent to 50 wt.%) possess increased strength while retaining high plasticity, low specific weight, and good corrosion resistance as reported by Mikheyev R. et al. [1]. This unique combination of properties makes the material suitable for making connecting rod components, bearings, and other wear-resistant parts [2; 3].

There are many AMCs manufacturing technologies. As mentioned by Nath H. et al. [4], these technologies can be divided into solid matrix and liquid matrix processes. Amosov A. et al. [5] note that the solid matrix processes are long and energy-consuming. On the other hand, conventional liquid matrix processes are unable to add a significant amount of reinforcing phase into the melt. This is due to low fluidity, and may result in undesirable chemical reactions between the matrix and the added components.

The new AMCs manufacturing technology is self-propagating, high-temperature synthesis (SHS). It is simple and suitable for virtually any melting furnace with a relatively low level of energy consumption. The SHS process is an exothermic reaction of initial reagents (powders of titanium and carbon or their compounds) in aluminum melt, producing titanium carbide as multiple dispersed particles [5—8].

Many recent studies have focused on increasing the fineness of the carbide phase particles and adding alloying elements to the matrix, since these have a positive effect on the AMCs properties. For example, Zhou D. et al. [9] studied the following aluminum melt (wt.%.): 5 Cu, 0.45 Mn, 0.3 Ti, 0.2 Cd, 0.2 V, 0.15 Zr, and 0.04 B. They added aluminum, titanium, and carbon nanotubes in the amounts of 0.1—1.0 wt.%. It was found that the formation of 0.5 wt.% of nanosized TiC particles increases composite strength to 540 MPa, and relative elongation, to 19 % (11 and 188 % growth compared to the initial matrix alloy). Tian W. et al. [10] used the same matrix to manufacture composites with 0.5 wt.% of TiC (particle size d = 97 nm), and 1, 3, and 5 wt.% of TiC (d = 1.88 μm). It was found that at t = 180 °C and under a 20 N load, the wear resistance of the nanoscale composite is 16.5 % higher than that of the composite reinforced with 5 wt.% of titanium carbide microparticles.

Amosov A. et al., Samara State Technical University [5] showed SHS process applicability to Al—TiC

mixtures (with powdered titanium and carbon). The reinforcing phase content is up to 20 % with an initial particle size of about 2—4 μm. Luts A. et al. [11] found that the addition of 5 wt.% of Na_2TiF_6 reduces the carbide particle size in the Al—10%TiC composite to ultra-fine (less than 1 μm). As a result, the strength after casting is increased by more than 80 % (from 115 to 200 MPa). The authors [12] manufactured Al—5%Cu—10%TiC, Al—5%Cu—2%Mn—10%TiC, and other heavy-duty composites containing an ultra-fine carbide phase.

Many recent works study alloy reinforcement by carbide phase both formed in the melt by SHS or added [13—15]. As a rule, the base metals are heat-treatable alloys. After reinforcement, the metal is treated with precipitation hardening (hardening + aging). Cho Y. et al. [16] showed that SHS applies to the highly dispersed carbide phase (6, 10, and 12 vol.%) in A2024 (Al—4.4%Cu—1.5%Mg). The sample containing 12 vol.% TiC, after extrusion, annealed at 400 °C for 20 h, quenched for 1 h at t = 500 °C, and aged at 190 °C for 8 h, showed the greatest increase in modulus of elasticity and tensile strength. This reached up to 93 GPa and 461 MPa, respectively. Ramakoteswara Rao V. et al. [17; 18] noted that a sample with 8 wt.% of TiC particles after adding 2—10 wt.% of TiC particles of about 2 μm to the AA7075 foundry alloy (Al—5.8%Zn—2.4%Mg), subsequent homogenization at t = 450 °C for 2 h, and aged at 121 °C for 24 h, increased its tensile strength from 400 to 600 MPa, and hardness, from 110 to 200 HV.

Nevertheless, some works indicate that heat treatment of AMCs does not always improve strength. Chen C. et al. [19] studied the aging behavior of the Al6061 alloy (Al—Mg—Si) reinforced with 2 % TiC particles (d = 40÷50 μm) at t = 160 °C. They established that the reinforcing particles prevent the formation of Guinier-Preston zones and strengthening metastable Mg—Si phases in the aluminum matrix. As a result, after T6 heat treatment, the max hardness (75.8 HV) of the Al6061—TiC composite was reached after 8 h of aging. This was much lower than that of the Al6061 matrix alloy after 18 h of aging (123 HV).

The review [20] summarizes the quenching and subsequent aging of Al—Cu—Mg—SiC, Al—Mg—Si—Cu—SiC, Al—Mg—Si—Cu—B4C, and Al—Zn—Mg—Cu—SiC AMCs reinforced by silicon carbide and manufactured with both solid matrix and liquid matrix processes. In general, the aging patterns of composites and aluminum alloys are different. The sequence of precipitation hardening phases and phase composition of the matrix material may vary, while the max AMCs hardness and strength are achieved in a shorter time. Furthermore, the hardening of the composites generally results in lower hardness than expected by "adding" the results of the precipitation hardening of the aluminum alloy and the matrix strengthening by reinforcing particles.

There are highly interesting studies which show that by changing the composition and structure of interfacial boundaries and by improving the matrix-to-filler bonding, it becomes possible to apply heat treatment to alloys considered unsuitable for precipitation hardening. One example is the study by Hashim J. et al. [21]. They reported that quenching at 550 °C for 20 min with hot water cooling and subsequent aging at 160 °C for 30 min of the non-heat-treatable AMg1 alloy with 2.5 wt.% SiC (d = 3 μm) increases the hardness to 1040—1200 HB, and tensile strength, to 153 MPa. One of the reasons may be the presence of magnesium in the alloy. Magnesium is often used as a surface active additive that segregates at the phase interface and reduces its energy [22].

For example, Contreras A. et al. [23] studied the interaction between titanium carbide substrate and Al—Mg melt at 900 °C. It was found that by increasing the Mg content from 1 to 20 % in the base aluminum, the wetting of the ceramic phase can be significantly improved by reducing the surface tension of aluminum drops. Magnesium additions also significantly strengthen aluminum alloys. In particular, Shu S. et al. [24] reported that the addition of 14 % Mg to SHS alloys manufactured by hot pressing increases the compressive strength of the Al—TiC composite by as much as 353 MPa.

This review confirms that magnesium significantly increases the efficiency of alloy hardening by adding titanium carbide. Gulyayev A. et al. [25] reported that such reinforcement is most appropriate for Al—Mg alloys (magnalium) which are known to have good formability and weldability, albeit relatively low strength and hardness. The most common alloys contain from 1 to 6 wt.% Mg, and micro amounts of other alloying elements (Fe, Si, Mn, Ti, Cu, Be, etc).

The Mg solubility in Al is 17.4 % at t = 450 °C and about 1.4 % at room temperature. Nevertheless, non-equilibrium solidification conditions in alloys containing as low as 1—2 % Mg may result in the formation of eutectic β phase inclusions of the Al_3Mg_2 (Mg_5Al_8) composition.

When solidified, transition metals form supersaturated solid solutions with aluminum [26; 27]. However, their low content does not lead to a significant increase in strength. Therefore, the formation of one more ultra-fine titanium carbide phase in magnalium may have a positive effect explained both by its hardening by reinforcing perticles and changing the sequence and the rate of structural transformations during the solidification and heat treatment caused by lattice micro-distortions.

The reinforcement results largely depend on the chemical composition of the alloy (the contents of magnesium and alloying elements). The purpose of this study is to obtain two composite materials by the SHS process and analyze the effects of heat treatment on their structure and properties. We studied the addition of titanium carbide to the AMg_2 (10%TiC) and AMg_6 (10%TiC) alloys.

Methods and materials

We used AMg2 (1520) and AMg6 (1560) alloy grades from Sammet (Russia) manufactured to GOST 4784-2019 as the melted matrix. In order to produce the charge mixture, we mixed powdered titanium (TPP-7 grade, TU 1715-449-05785388 Spec.) and carbon (P-701, GOST 7585-86) in a stoichiometric ratio for the Ti + C = TiC SHS reaction with Na_2TiF_6 (GOST 10561-80) added in amount of 5 % of the charge weight. The mixture was then divided into 3 equal parts wrapped in aluminum foil. Each was added to the AMg2 or AMg6 melts at 900 °C in a graphite crucible placed in a PS-20/12 melting furnace (made in Russia), in order to induce the SHS reaction and make the desired composites.

In the aims of studying the microstructure, we etched the samples with a 50 % HF + 50 % HNO_3 solution for 10—15 sec. Then we analyzed the samples with a JSM-6390A scanning electron microscope (Jeol, Japan) with a JSM-2200 energy-dispersive spectroscopy (EDS) module.

We also used XRD for phase identification. The XRD instrument was an ARL X'trA *X*-ray diffraction system (Thermo Scientific, Switzerland) with the CuK_α radiation and continuous scanning in the 2θ = = 20÷80° angle range at 2 deg/min. The HighScore Plus software (PANalytical B.V., Netherlands) was used to analyze the XRD patterns. The AMCs samples were heat treated in a SNOL lab furnace (temperature up to 1300 °C).

We measured the sample density by hydrostatic weighing on a VK-300 scale (made in Russia), accuracy class 4, GOST 20018-74. The demineralized water density was assumed to be 0.99733 g/cm^3 at the room air temperature of 24 °C. For dimensional control and composition analysis, we used a MIM 43 optical metallographic microscope (made in Russia) and the SIAMS 800 image processing software.

We measured AMCs electrical conductivity using a VE-26NP eddy current structurescope (made in Russia) according to GOST 27333-87. The hardness of the samples was measured using a TSh-2M hardness tester (made in Russia) according to GOST 9012-59. The impression diameter was defined using a Motic DM-111 microscope (made in Russia) and the Motic Educator image analysis software. For sample microhardness testing, a PTM-3 standard microhardness tester (made in Russia) was used according to GOST 9450-76. The instrument drives a square diamond pyramid (136° vertex angle). The penetrator load was 100 g.

We performed compression tests on the type III samples (d_0 = 20 mm) according to GOST 25.503-97. The relative strain and reduction ratio was established as specified in GOST 8817-82.

Corrosion resistance was evaluated according to GOST 13819-68 in a Coat Test 3.3.150.150 autoclave under the following conditions: 5 % NaCl aqueous solution; CO_2 (1 Pa) + H_2S (0.5 MPa) + N_2 (3.5 MPa) gas phase at 80 °C 240 h: 5 MPa total pressure. The corrosion resistance factors were calculated according to GOST 9.908-85. We used a Universal-1B tribology tester (made in Russia) for tribology testing as follows:

— friction type: boundary friction (sliding);
— block-on-ring contact arrangement;
— counterbody material: 40H grade steel;

— lubricant: Shell Helix Ultra SAE 5W-40 synthetic engine oil;
— normal contact load: 380 N;
— counterbody rpm: 600 (average linear velocity at the contact area: 0.157 m/s);
— test period: 30 min (or until seizure).

Results and discussion

The powders mixtures used to make both composites in the AMg2 or AMg6 melts at 900 °C produced an intense, rapid SHS reaction with bright flashes. The fractures of the synthesized samples were homogeneously gray and lacked any foreign inclusions or residues of unreacted charge.

Composite manufacturing and heat treatment AMg2–10%TiC

Figure 1 shows the microstructure of AMg2—10%TiC composite manufactured with SHS. The process produces a large number of both small sintered agglomerates, and ultra-fine rounded particles larger than 180 nm. XRD analysis revealed the presence of Al, Ti, C, and Mg (Fig. 2). XRD analysis also identified the presence of the required TiC phase (Fig. 3). EDS analysis indicated a presence of Mg, so the β-phase may be also present but its amount is too small to be detected by XRD.

XRD processing identified the presence of a carbide phase (8 wt.%). This is an acceptable level, considering some inhomogeneity of its distribution. The average grain size reduced from 9.64 (±4.82) μm in the matrix to 1.31 (±0.056) μm in the composite material. It confirms the modifying effect of the carbide phase particles. Measurements showed an increase in hardness from 509 HB for the AMg2 casting alloy to 594 HB for the AMg2—10%TiC composite. It matches the hardness of the hardened AMg2 alloy.

We can conclude that, due to the absence of plastic deformation, the presence of highly dispersed carbide particles increases the hardness.

Next we selected the optimal temperature and time for heat treatment. As noted above, the lean AMg2 alloy does not undergo precipitation hardening after quenching. It consists mainly of a solid solution of magnesium in aluminum. However, as was shown above and by Kurganova Y. et al. [21], heat treatment of the AMg1 composite with a fine phase can produce some new effects.

Taking all the factors into account, we selected the following heat treatment modes: 130, 150, 180, and 350 °C for 1, 2, and 3 h with subsequent still air cooling [28]. The hardness was a quantitative criterion aimed at evaluating the effects of heat treatment. Figure 4 presents the results. The highest value of 676 HB (compared to the initial 594 HB for the foundry composite) is achieved after heating at 150 °C for 2—3 h. Heating at 350 °C does not affect the hardness.

The microstructure and EDS analysis of the AMC samples with the highest hardness (Figs. 5 and 6) show that the carbide particle sizes and chemical composi-

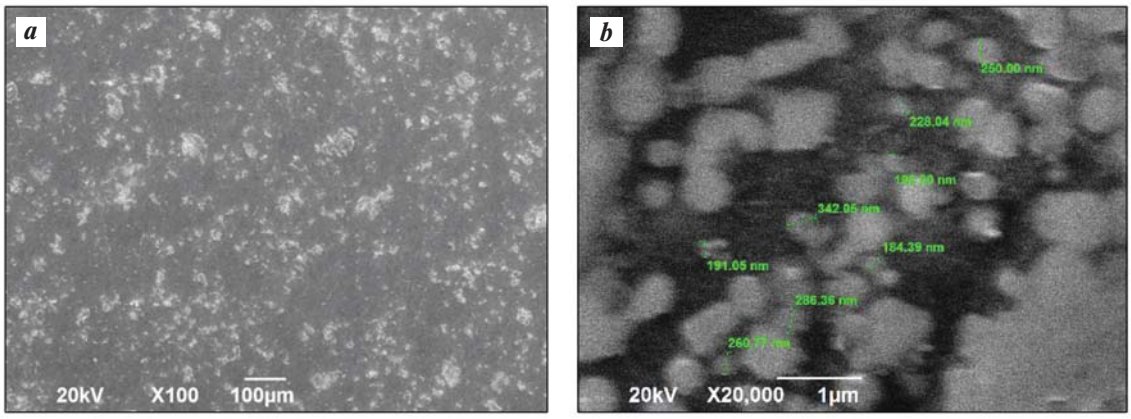

Fig. 1. SEM image of the AMg2–10%TiC composite
a – ×100 magnification, ***b*** – ×20000 magnification

Рис. 1. Микроструктура композиционного материала АМг2–10%TiC
a – увеличение ×100, ***b*** – ×20000

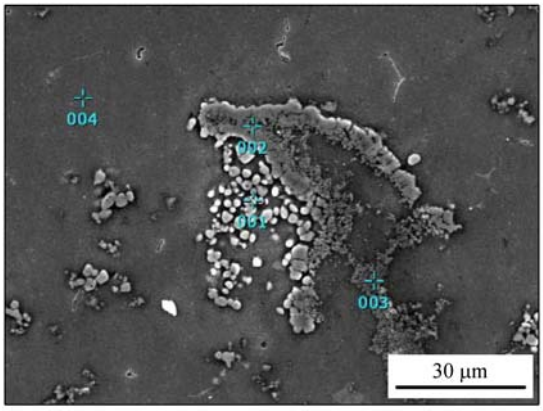

Marker number	Element content, wt.%				
	C	Al	Ti	Mg	F
001	28.01	14.27	57.72	0	0
002	17.97	38.17	38.01	3.49	2.36
003	17.82	47.91	28.71	3.92	1.65
004	0	93.93	0	6.07	0

Fig. 2. EDS analysis of the AMg2–10%TiC composite

Рис. 2. Результаты МРСА композиционного материала AMr2–10%TiC

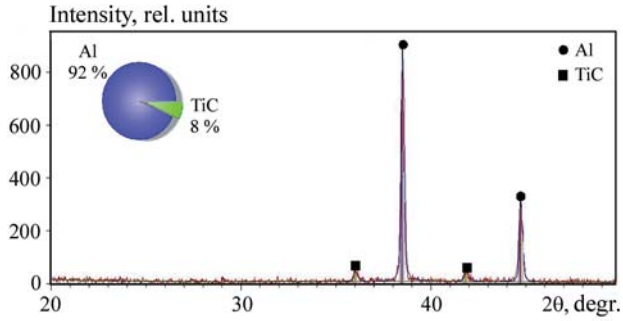

Fig. 3. XRD pattern of the AMg2–10%TiC composite

Рис. 3. Дифрактограмма композиционного материала AMr2–10%TiC

tion are not affected. However, EDS indicates that the result of heat treatment leads both to the appearance of elemental magnesium and XRD peaks of the Al_3Mg_2 β-phase in the amount of 3 wt.%. This means an additional release of magnesium from the solid solution of aluminum (Fig. 7).

We made the following assumption about the sequence of structural transformations before and after heat treatment based on the experimental data. Imme-

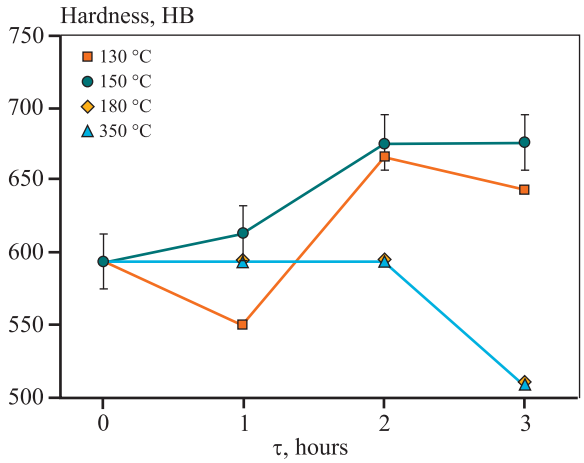

Fig. 4. The hardness variations of the AMg2–10%TiC composite after heat treatment at different temperatures

Рис. 4. Изменение твердости композиционного материала AMr2–10%TiC после дополнительного нагрева при разных температурах

diately after pouring the composite into the mould and during the solidification cooling, the presence of a large number of carbide particles distort the lattice of the matrix and cause high internal stresses. This is due to the formation of the Mg_2Si, $Al_6(Fe, Mn)$, $Al_{15}(Fe, Mn)_2Si_3$ crystallization phases [29]. After solidification, a partial precipitation of the β-phase from the solid solution is possible.

It should be noted that the presence of the Al_3Mg_2 phase can decrease the strength and corrosion resistance, since it precipitates as continuous chains along the grain boundaries [29]. In this case, the large number of dispersed carbide particles prevents the formation of such continuous precipitates, while individual intermetallic β-phase inclusions may increase the hardness. Additional heating at t = 150 °C while the internal stress still applies facilitates the diffusion. Subsequent cooling in air leads to an additional β-phase release, increasing hardness.

There is no change to hardness after heating to 350 °C (see Fig. 4) because a solid solution is formed throughout the entire alloy volume at this temperature. Cooling leads to the same processes as after SHS, and the initial hardness is restored.

Composite manufacturing and heat treatment AMg6–10%TiC

Figure 8 shows the microstructure of the AMg6–10%TiC composite. Compared to the previous case,

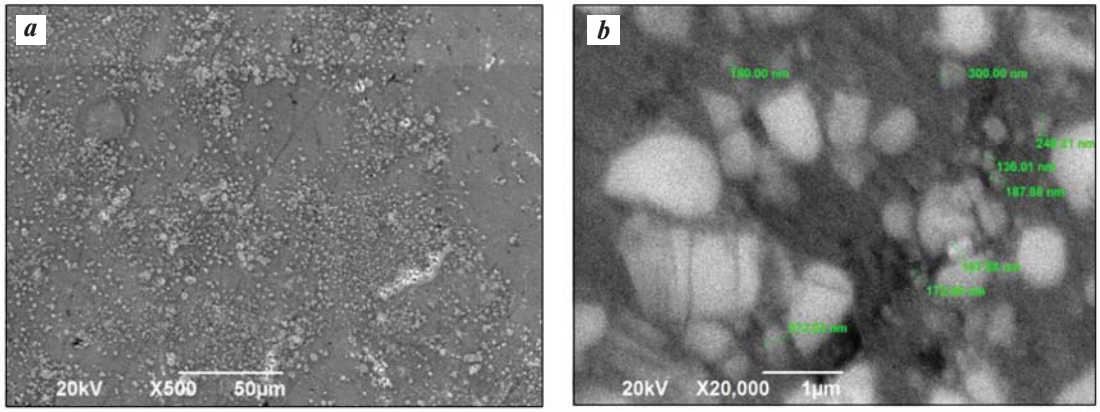

Fig. 5. SEM image of the AMg2–10%TiC composite after additional heating at t = 150 °C for 2 h
a – ×500 magnification, ***b*** – ×20000 magnification

Рис. 5. Микроструктура композиционного материала АМг2–10%TiC после дополнительного нагрева при t = 150 °C в течение 2 ч
a – увеличение ×500, ***b*** – ×20000

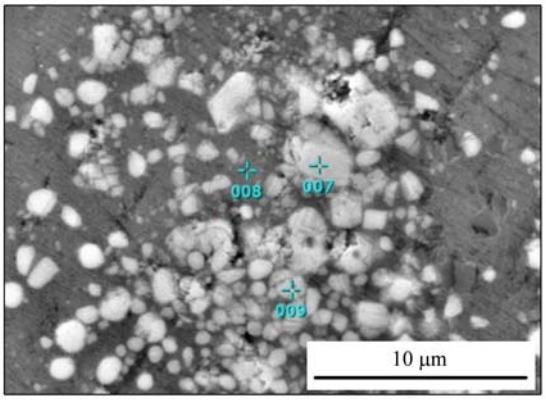

Marker number	Element content, wt.%			
	C	Al	Ti	Mg
007	22.04	13.54	63.19	1.22
008	14.60	75.90	4.88	4.60
009	29.00	38.44	29.89	2.67

Fig. 6. EDS analysis of the AMg2–10%TiC composite after additional heating at t = 150 °C for 2 h

Рис. 6. Результаты МРСА композиционного материала АМг2–10%TiC после дополнительного нагрева при t = 150 °C в течение 2 ч

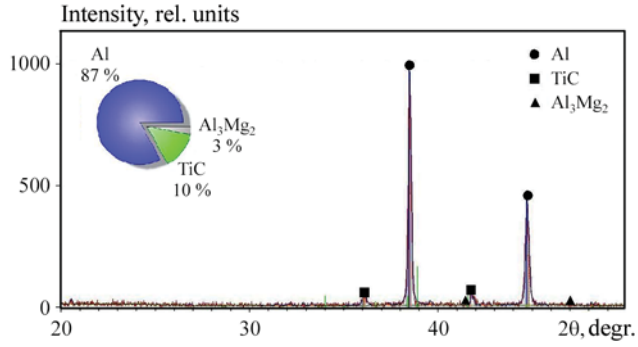

Fig. 7. XRD pattern of the AMg2–10%TiC composite after additional heating at t = 150 °C for 2 h

Рис. 7. Дифрактограмма композиционного материала АМг2–10%TiC после дополнительного нагрева при t = 150 °C в течение 2 ч

carbide phase particles exceeding 130 nm are distributed more uniformly over the alloy volume. This can be explained by the higher magnesium content and, consequently, their higher wettability, and better assimilation.

XRD analysis indicates the presence of the TiC target phase (Figs. 9 and 10), while the presence of magnesium suggests the presence of the β-phase.

The XRD pattern analysis confirms the presence of a carbide phase in the amount of 10 wt.%. Average grain size decreased from 15.8 (±34.3) μm in the matrix alloy to 10.6 (±3.56) μm in the composite. The process increases the hardness from 830 to 909 HB for AMg6—10%TiC casting alloy.

The AMg6 alloy is not a conventional precipitation hardened material. However, the high magnesium content provides the highest strength among all other magnalium alloys. The alloy is usually hardened or is subjected to recrystallization annealing in the

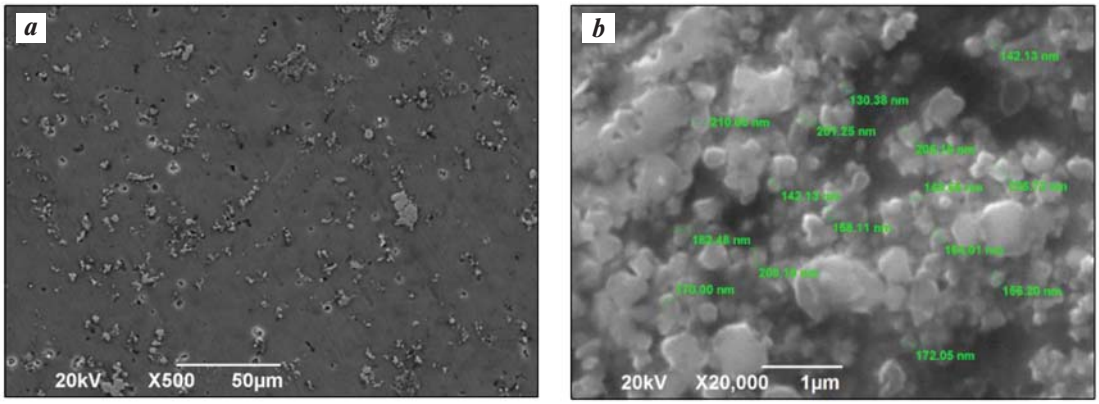

Fig. 8. SEM image of the AMg6–10%TiC composite
a – ×500 magnification, ***b*** – ×20000 magnification

Рис. 8. Микроструктура композиционного материала АМг6–10%TiC
a – увеличение ×500, ***b*** – ×20000

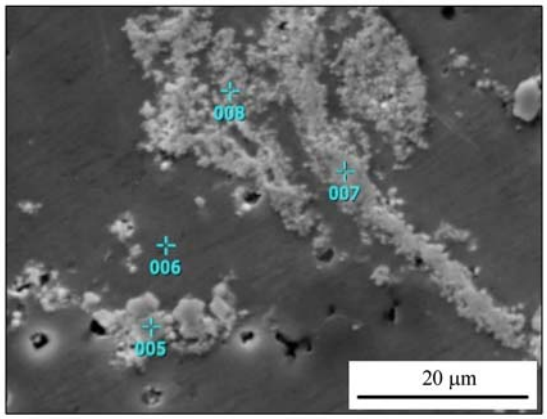

Marker number	Element contents, min., wt.%			
	Al	Ti	C	Mg
005	4.43	90.18	4.74	0.66
006	90.56	0.22	0.15	9.06
007	5.13	88.60	5.46	0.81
008	40.24	51.14	2.76	5.86

Fig. 9. EDS analysis of the AMg6–10%TiC composite

Рис. 9. Результаты МРСА композиционного материала АМг6–10%TiC

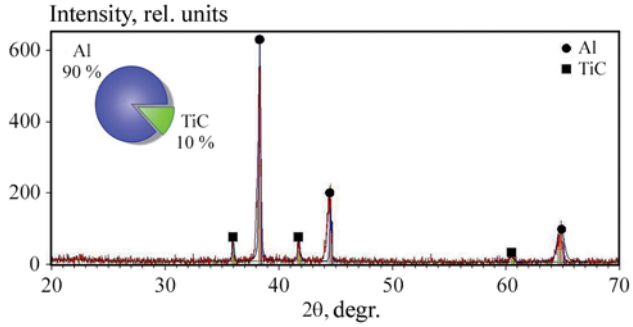

Fig. 10. XRD pattern of the AMg6–10%TiC composite

Рис. 10. Дифрактограмма композиционного материала АМг6–10%TiC

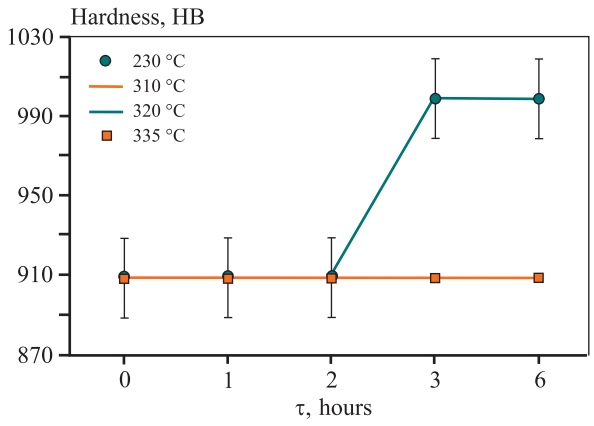

Fig. 11. The hardness changes of the AMg6–10%TiC composite after additional heating at different temperatures

Рис. 11. Изменение твердости композиционного материала АМг6–10%TiC после дополнительного нагрева при разных температурах

310—335 °C temperature range, in order to increase its ductility, with furnace holding time from 30 min to 3 h and air cooling [26].

Kishchik M. et al. [30] studied the effects of different heterogenization annealing modes for the 1565ch alloy containing 5.1—6.0 wt.% Mg and alloying Zr. The tem-

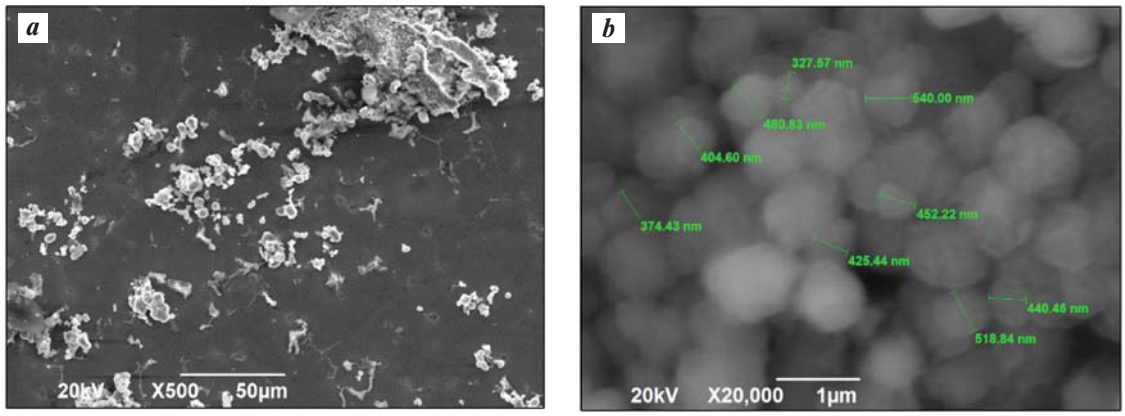

Fig. 12. SEM image of the AMg6–10%TiC composite after additional heating at t = 230 °C for 3 h
a – ×500 magnification, ***b*** – ×20000 magnification

Рис. 12. Микроструктура композиционного материала АМг6–10%TiC после дополнительного нагрева при t = 230 °C в течение 3 ч
a – увеличение ×500, ***b*** – ×20000

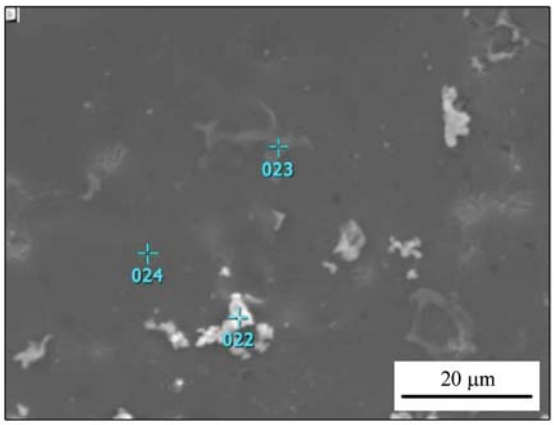

Marker number	Element contents, min., wt.%					
	Al	Ti	C	Mg	Mn	Fe
022	9.92	85.04	3.73	1.31	–	–
023	80.86	–	–	6.75	3.86	8.54
024	93.41	–	–	6.59	–	–

Fig. 13. EDS analysis of the AMg6–10%TiC composite after additional heating at t = 230 °C for 3 h

Рис. 13. Результаты МРСА композиционного материала АМг6–10%TiC после дополнительного нагрева при t = 230 °C в течение 3 ч

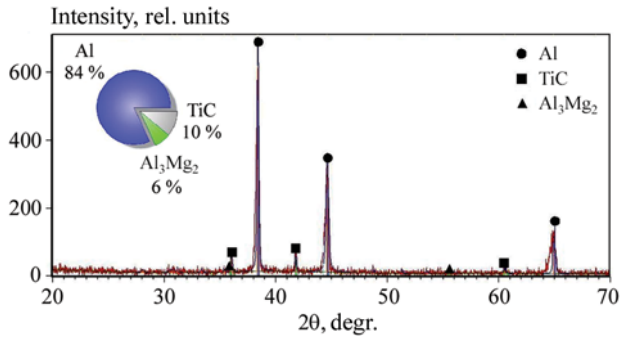

Fig. 14. XRD pattern of the AMg6–10%TiC composite after additional heating at t = 230 °C for 3 h

Рис. 14. Дифрактограмма композиционного материала АМг6–10%TiC после дополнительного нагрева при t = 230 °C в течение 3 ч

perature varied from 130 to 280 °C, and the holding time from 1 to 12 h. The results showed that the formation of homogeneously distributed individual β-phase particles during annealing at t = 230 °C with a 6 h holding time produces a fine-grained structure, and leads to the highest hardness gain.

Considering the above, we selected the following treatment mode for the AMg6—10%TiC composite: heating at t = 230 °C for 1, 3, and 6 h at 310, 320, and 335 °C for 1, 2, and 3 h. Fig. 11 shows the measured hardness values. It indicates that heat treatment in the t = 310÷335 °C range does not increase hardness. Its highest value (999 HB) is achieved after holding at t = 230 °C for 3 and 6 h.

Just like with the first alloy, additional heating at a temperature close to the solubility line contributes to higher hardness.

Figures 12—14 shows the XRD, EDS, and microstructural analysis results of the sample with the highest hardness. XRD analysis showed the presence of not only Al, Ti, C, and Mg, but also Mn and Fe. It may indicate the presence of intermetallic and ceramic phases formed during solidification. However, the primary phase formed after heating is Al_3Mg_2 in the amount of 6 wt.%. It accounts for the hardness increase (Fig. 14).

Properties of AMg2–10%TiC and AMg6–10%TiC composites

We compared the properties of the original cold-hardened alloys with index N, composites without heat treatment (No HT), and composites after additional heating resulting in the highest hardness.

The SHS process is characterized by significant outgassing which can adversely affect the composite properties. For this reason, we initially determined the density (ρ_{test}) and porosity (P) of the samples (Table 1). The ρ_{test} values of the AMCs are slightly higher than those of the original matrix alloys. This confirms the presence of a carbide phase with $\rho = 4.92$ g/cm^3. The reference density (ρ_{ref}) was calculated for the AMCs containing 10 % TiC.

The comparison of the reference and experimental density values indicates that the porosity of the SHS cast samples does not exceed 1%. Heat treatment reduces it to zero, confirming higher adhesive bonding at the phase interfaces.

Then we studied the electrical conductivity. It is an important characteristic of all aluminum alloys (Table 2).

Pan S. et al. [31] reported that only AMCs reinforced with ultra-fine nanophases (such as CNTs, graphene, etc.) can have high electrical conductivity. The possibility of making a conductive material con-

Table 1. **Density and porosity of the original alloys and composites**

Таблица 1. Плотность и пористость сплавов и композиционных материалов

Sample composition	ρ_{test}, g/cm^3	ρ_{ref}, g/cm^3	P, %
AMg2N	2.69	–	–
AMg2—10%TiC (no HT)	2.82	2.797	0.82
AMg2—10%TiC (heating to 150 °C, 2 h)	2.82	2.826	0
AMg6N	2.64	–	–
AMg6—10%TiC (no HT)	2.768	2.739	1
AMg6—10%TiC (heating to 230 °C, 3 h)	2.768	2.768	0
AMg6—10%TiC (heating to 230 °C, 6 h)	2.768	2.768	0

Table 2. **Electrical conductivity of alloys and composites**

Таблица 2. Электропроводность сплавов и композиционных материалов

Sample composition	Electrical conductivity, MSm/m
AMg2N	19.7
AMg2—10%TiC (no HT)	15.4
AMg2—10%TiC (heating to 150 °C, 2 h)	16.6
AMg6N	14.5
AMg6—10%TiC (no HT)	10.57
AMg6—10%TiC (heating to 230 °C, 3 h)	11.2
AMg6—10%TiC (heating to 230 °C, 6 h)	10.98

Table 3. **Mechanical properties and manufacturability of the alloys and composites**

Таблица 3. Механические и технологические свойства сплавов и композиционных материалов

Sample composition	$\sigma_в^*$, MPa	ε^*, %	Hardness, HB	Microhardness, HV	Relative strain,%	Reduction ratio
AMg2N	290	69.19	594	608	32	1.48
AMg2–10%TiC (no HT)	271	59.7	594	736	25	1.33
AMg2–10%TiC (heating to 150 °C, 2 h)	288	61.5	676	745	29	1.41
AMg6N	449	32	830	991	44	1.8
AMg6–10%TiC (no HT)	403	19	909	1020	43	1.62
AMg6–10%TiC (heating to 230 °C, 3 h)	395	14	999	1069	43	1.75

* Uniaxial compression tests.

Table 4. **Corrosion resistance of alloys and composites**

Таблица 4. Коррозионная стойкость сплавов и композиционных материалов

Sample composition	Weight loss, g	Weight loss per unit area, kg/m^2	Sample thickness change, m	Corrosion rate, g/(cm^2·h)	Corrosion depth rate, mm/year
AMg2N	0.6187	0.160	0.058	0.666	0.0021
AMg2–10%TiC (no HT)	0.3686	0.095	0.035	0.416	0.0014
AMg2–10%TiC (heating to 150 °C, 3 h)	0.418	0.108	0.038	0.450	0.0014
AMg6N	0.8935	0.231	0.082	0.962	0.003
AMg6–10%TiC (no HT)	0.5826	0.151	0.057	0.627	0.0021
AMg6–10%TiC (heating to 230 °C, 3 h)	0.8063	0.208	0.075	0.868	0.0027

taining a titanium carbide reinforcing phase is still under study.

The values measured are slightly lower than those of the original alloys due to the presence of the carbide phase. Pan S. et al. [32] confirm this. They reported that an AMC with 3.68 vol.% TiC and aluminum matrix has a higher electrical resistance and, consequently, lower conductivity.

We measured the ultimate strength (σ_B) and relative strain (ε) with the subsequent compression tests (Table 3). It was found that both values for the AMg2—10%TiC composite are slightly lower than the original matrix alloy values. For AMg6—10%TiC the decrease is more significant. This is probably due to the extensive formation of the β-phase in the AMg6 alloy. The accumulation of clusters is more difficult to prevent. Furthermore, magnesium, as a highly active metal, can form compounds with oxygen. At low Mg content, $MgAl_2O_4$ is formed, and at high content, MgO [33].

Rafalsky I. et al. [34] studied the effects of adding 2 wt.% Mg on the structure of Al—1%Ti—10%SiC

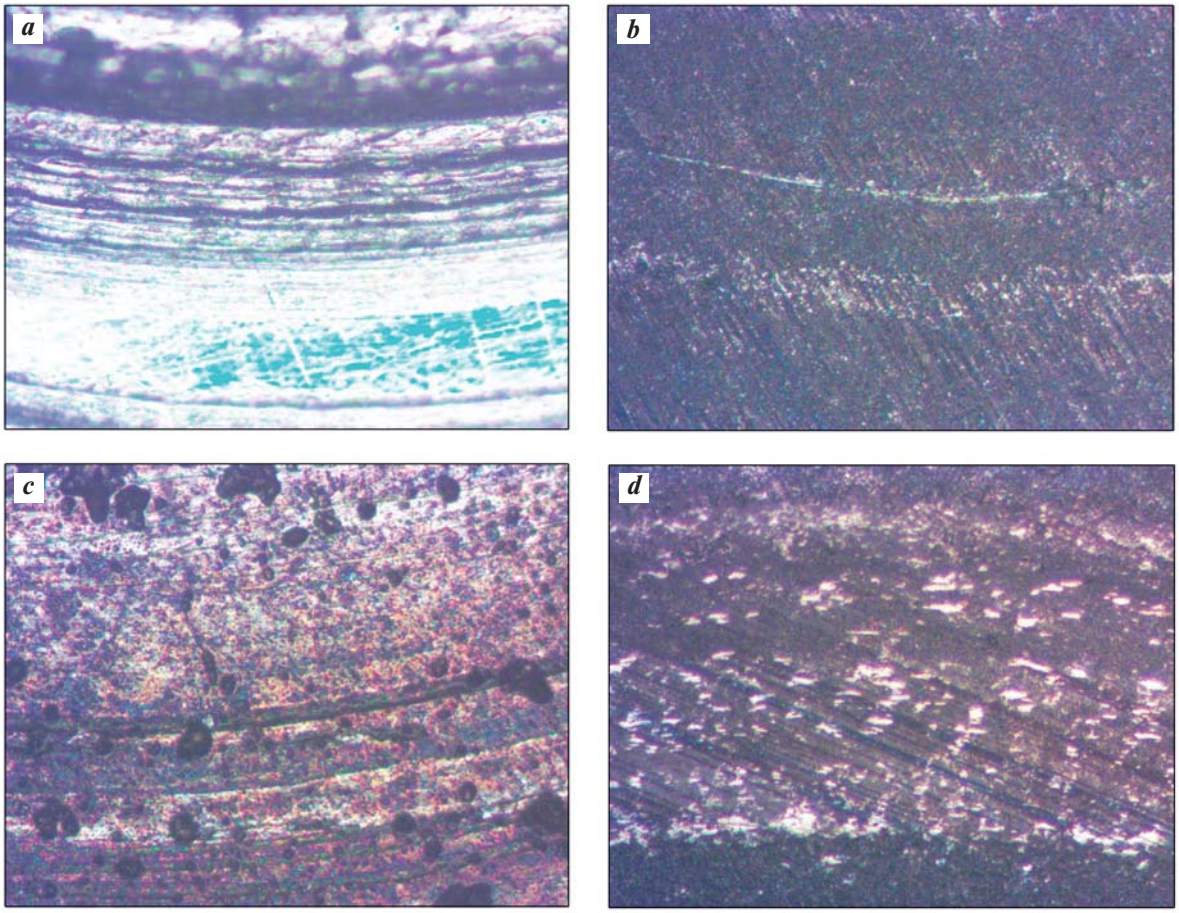

Fig. 15. Friction surface of the AMCs samples
a – AMg2N; ***b*** – AMg2–10%TiC (heating to 150 °C, 3 h); ***c*** – AMg6N; ***d*** – AMg6–10%TiC (heating to 230 °C, 3 h)

Рис. 15. Вид поверхности трения образцов АМКМ
a – АМг2Н; ***b*** – АМг2–10%TiC (нагрев до 150 °C, 3 ч); ***c*** – АМг6Н; ***d*** – АМг6–10%TiC (нагрев до 230 °C, 3 ч)

Table 5. **Tribological tests**

Таблица 5. Результаты сравнительных триботехнических испытаний

Sample composition	Wear rate, μm/h	Friction coefficient	Self-heating temperature, °C
AMg2N	37.6±5.2	up to 0.3	71
AMg2–10%TiC (no HT)	6.4±1.6	0.11–0.12	65
AMg2–10%TiC (heating to 150 °C, 2 h)	4.0±1.3	0.07–0.08	56
AMg6N	15.5±4.1	0.13–0.15	70
AMg6–10%TiC (no HT)	3.5±0.6	0.07–0.09	59
AMg6–10%TiC (heating to 230 °C, 3 h)	4.2±1.2	0.08–0.10	66

composite manufactured by mixing at 850—900 °C. The final material contains individual, extended film-like clusters of $MgAl_2O_4$. The presence of Mg-containing inclusions at the phase interfaces can minimize the effect of higher wettability, and contribute to strength reduction. Mikheev R. et al. [35] also showed that by adding 10 wt.% of TiC 40—100 μm reinforcing particles to the AK12M2MgN, the aluminum alloy decreases compressive strength from 489 to 470 MPa, while the relative strain drops from 17.01 to 12.65 %. Therefore, an insignificant decrease in these properties is expected in composites reinforced with titanium carbide. Furthermore, the hardness values of AMg2—10%TiC and AMg6—10%TiC increase by 12 and 17 %, and the microhardness values increase by 18 and 7 %, respectively.

During the upsetting test (Table 3), we loaded the samples to the maximum. The samples of AMg2 and AMg6 matrix alloys were deformed by 32 and 44 % without cracking. The test was stopped upon cracking. The cracks always occurred not in the sample body, but on its circumference. It was found that the AMCs after heating have better strain and reduction ratio values than the original alloys. These values are almost identical to the matrix alloy values. The ε = 29 and 43 % measured values are assumed to be the strain limits for the AMCs samples. This is a satisfactory result, since in real-life applications magnalium alloys are not subjected to strains exceeding 30 % which leads to a decrease in the plasticity. It can also create instability of mechanical and corrosion resistance properties [26].

High corrosion resistance is one of the key advantages of magnalium alloys. After annealing, the corrosion resistance is 3 points (Perelygin Yu. et al. [36]). We also measured this property (Table 4). All the AMCs samples have a corrosion depth rate of 0.001—0.005 mm/year. It matches that of the matrix alloys and means that the AMCs are highly resistant.

Finally, we compared the tribological properties of the investigated materials. The samples of the original AMg2 matrix alloy showed wear with seizures and abrasive wear. It leads to rapid destruction of the surface layer. The AMg6 sample featured unstable friction torque values, indicating undesirable effects in the friction contact area (Fig. 15, *a*, *b*).

All the AMCs samples showed better tribological properties such as good mechanical conformability, halving the friction coefficient, and up to 88 % wear rate reduction (Fig. 15, *c*, *d* and Table 5).

Conclusion

This study showed that heat treatment of composites based on aluminum-magnesium matrix alloys reinforced with ultra-fine titanium carbide is a promising method of controlling the composite structure and properties, although the original matrix alloys are not-heat-treatable.

It was found that SHS of the AMg2—10%TiC composite with subsequent heating to 150 °C maintains compressive strength, deformability, and corrosion resistance (virtually identical to the original hardened matrix alloy values). Furthermore, hardness is increased by 12 %, and microhardness by 18 %. The friction coefficient is reduced by at least 75 %, and the wear rate by 88 %.

It was found that SHS of the AMg6—10%TiC composite with subsequent heating to 230 °C reduces compressive strength by 12 %, while deformability and corrosion resistance are still acceptable. Hardness is increased by 17 %, and microhardness by 7 %. The friction coefficient is halved and the wear rate is reduced by 72 %.

The liquid matrix SHS process with subsequent heat treatment of aluminum-magnesium alloy composites hardened with ultra-fine titanium carbide can produce light and wear-resistant materials.

References

1. Mikheyev R.S., Chernyshova T.A. Aluminum-matrix composite materials with carbide hardening for solving problems of new technology. Moscow: RFFI, 2013. 353 p. (In Russ.).
   Михеев Р.С., Чернышова Т.А. Алюмоматричные композиционные материалы с карбидным упрочнением для решения задач новой техники. М.: Издание РФФИ, 2013. 353 с.
2. Sethi V. Effect of aging on abrasive wear resistance of silicon carbide particulate reinforced aluminum matrix composite. USA: University of Cincinnaty, 2007. 114 p.
3. Panfilov A.A., Prusov E.S., Kechin V.A. Problems and prospects for the development of production and application of aluminum matrix composite alloys. *Trudy Nizhegorodskogo gosudarstvennogo tekhnicheskogo universiteta imeni R.Ye. Alekseyeva*. 2013;2(99):210—217. (In Russ.).

Панфилов А.А., Прусов Е.С., Кечин В.А. Проблемы и перспективы развития производства и применения алюмоматричных композиционных сплавов. *Труды Нижегородского государственного технического университета им. Р.Е. Алексеева*. 2013; 2(99):210—217.

4. Nath H., Amosov A.P. SHS amidst other new processes for in-situ synthesis of Al-matrix composites: A review. *International Journal of Self-Propagating High-Temperature Synthesis*. 2016;(25):50—58. http://doi.org/10.3103/S106138621601009X
5. Amosov A.P., Luts A.R., Latukhin E.I., Ermoshkin A.A. Application of SHS processes for in situ production of aluminum-matrix composite materials discretely reinforced with nanoscale titanium carbide particles: Overview. *Russian Journal of Non-Ferrous Metals*. 2016;57(2):106—112. http://doi.org/10.3103/S1067821216020024
   Амосов А.П., Луц А.Р., Латухин Е.И., Ермошкин А.А. Применение процессов СВС для получения *in situ* алюмоматричных композиционных материалов, дискретно армированных наноразмерными частицами карбида титана: Обзор. *Известия вузов. Цветная металлургия*. 2016;(1):39—49. http://doi.org/10.17073/0021-3438-2016-1-39-49
6. Pramod S.L., Bakshi S.R., Murty B.S. Aluminum-based cast in situ composites: A review. *Journal of Materials Engineering and Performance*. 2015;24(6):2185—2207. http://doi.org/10.1007/s11665-015-1424-2
7. Pandey U., Purohit R., Agarwal P., Dhakad S.K., Rana R.S. Effect of TiC particles on the mechanical properties of aluminium alloy metal matrix composites (MMCs). *Materials Today: Proceedings*. 2017;4:5452—5460. http://doi.org/10.1016/j.matpr.2017.05.057
8. Chaubey A.K., Prashanth K.G., Ray N., Wang Z. Study on in-situ synthesis of Al—TiC composite by self — propagating high temperature synthesis process. *Materials Science: An Indian Journal*. 2015;12(12): 454—461.
9. Zhou D., Qiu F., Jiang Q. The nano-sized TiC particle reinforced Al—Cu matrix composite with superior tensile ductility. *Materials Science and Engineering:A*. 2015;622:189—193. http://doi.org/10.1016/j.msea.2014.11.006
10. Tian W.S., Zhao Q.L., Zhao C.J., Qiu F., Jiang Q.C. The dry sliding wear properties of nano-sized TiCp/Al—Cu composites at elevated temperatures. *Materials*. 2017;10:939. http://doi.org/10.3390/ma10080939
11. Luts A.R., Amosov A.P., Ermoshkin A.A., Ermoshkin A.A., Nikitin K.V., Timoshkin I.Y. Self-propagating high-temperature synthesis of highly dispersed titanium-carbide phase from powder mixtures in the aluminum melt. *Russian Journal of Non-Ferrous Metals*. 2014;55(6):606—612. http://doi.org/10.3103/S1067821214060169
    Луц А.Р., Амосов А.П., Ермошкин А.А., Ермошкин А.А., Никитин К.В., Тимошкин И.Ю. Самораспространяющийся высокотемпературный синтез высокодисперсной фазы карбида титана из смесей порошков в расплаве алюминия. Известия вузов. *Порошковая металлургия и функциональные покрытия*. 2013;(3):28—35.
12. Luts A.R., Amosov A.P., Latukhin E.I., Rybakov A.D., Novikov V.A., Shipilov S.I. Self-propagating high-temperature synthesis of (Al—2% Mn)—10% TiC and (Al—5% Cu—2% Mn)—10% TiC nanostructured composite alloys doped with manganese powder. *Russian Journal of Non-Ferrous Metals*. 2019;60(4):413—421. http://doi.org/10.3103/S1067821219040072
    Луц А.Р., Амосов А.П., Латухин Е.И., Рыбаков А.Д., Новиков В.А., Шипилов С.И. Самораспространяющийся высокотемпературный синтез наноструктурных композиционных сплавов (Al—2%Mn)—10%TiC и (Al—5%Cu—2%Mn)—10%TiC при легировании порошковым марганцем. *Известия вузов. Порошковая металлургия и функциональные покрытия*. 2018;(3):30—40. http://doi.org/10.17073/1997-308X-2018-3-30-40
13. Sai Chaitanya Kishore D., Prahlada Rao K., Mahamani A. Investigation of cutting force, surface roughness and flank wear in turning of in situ Al6061—TiC metal matrix composite. *Procedia Materials Science*. 2014;6:1040—1050. http://doi.org/10.1016/j.mspro.2014.07.175
14. Kareem A., Qudeiri J.A., Abdudeen A., Ahammed T., Ziout A. A review on AA 6061 metal matrix composites produced by stir casting. *Materials*. 2021;14(1):175. http://doi.org/10.3390/ma14010175
15. Krishna Prasad S., Dayanand S., Rajesh M., Nagaral M., Auradi V., Selvaraj R. Preparation and mechanical characterization of TiC particles reinforced Al7075 alloy. *Advances in Materials Science and Engineering*. 2022;1:1—11. http://doi.org/10.1155/2022/7105189
16. Cho Y.H., Lee J.M., Kim S.H. Al—TiC Composites fabricated by a thermally activated reaction process in an al melt using Al—Ti—C—CuO powder mixtures:

Pt. II. Microstructure control and mechanical properties. *Metallurgical & Materials Transaction*s. 2015;46A:1374—1384. http://doi.org/10.1007/s11661-014-2476-x

17. Ramakoteswara Rao V., Ramanaiah N., Sarcar M.M. Mechanical and tribological properties of AA7075—TiC metal matrix composites under heat treatment (T6) and cast conditions. *Journal of Materials Research and Technology*. 2016;5(4):377—383. http://doi.org/10.1016/j.jmrt.2016.03.011
18. Ramakoteswara Rao V., Ramanaiah N., Sarcar M.M. Dry sliding wear behavior of Al7075 reinforced with titanium carbide (TiC) particulate composites. In: *Proceedings of Int. Conf. on Advances in Materials, Manufacturing and Applications (AMMA 2015)* (2015, April 9—11). P. 39—44. URL: https://www.researchgate.net/publication/279868886_Dry_Sliding_Wear_Behavior_of_Al7075_Reinforced_with_Titanium_Carbide_TiC_Particulate_Composites (accessed: 21.03.2023).
19. Chen C.L., Lin C.H. A Study on the aging behavior of Al6061 composites reinforced with Y_2O_3 and TiC. *Metals*. 2017;7 (11):7—11. http://doi.org/10.3390/met7010011
20. Kurbatkina E.I., Shavnev A.A., Kosolapov D.V., Gololobov A.V. Features of thermal treatment of composite materials with aluminum matrix (Review). *Trudy VIAM*. 2017;11:82—97. URL: http://viam-works.ru/ru/articles?year=2017&num=11 (accessed: 21.03.2023). (In Russ.). http://dx.doi.org/ 10.18577/2307-6046-2017-0-11-9-9
Курбаткина Е.И., Шавнев А.А., Косолапов Д.В., Гололобов А.В. Особенности термической обработки композиционных материалов с алюминиевой матрицей (обзор). *Труды ВИАМ*. 2017;11:82—97. URL: http://viam-works.ru/ru/articles?year=2017&num=11 (дата обращения: 21.03.2023). http://dx.doi.org/ 10.18577/2307-6046-2017-0-11-9-9
21. Kurganova Y.A. Development and applications of dispersion strengthened aluminum matrix composite materials in mechanical engineering: Abstract of dissertation of Dr. Sci. (Eng.). Moscow: IMET RAS, 2008. (In Russ.).
Курганова Ю.А. Разработка и применение дисперсно-упрочненных алюмоматричных композиционных материалов в машиностроении: Автореф. дис. ... д.т.н. М.: ИМЕТ РАН, 2008.
22. Hashim J. The production of cast metal matrix composite by a modified stir casting method. *Jurnal Teknologi*. 2001;35(1):9—20. http:// doi.org/10.11113/jt.v35.588
23. Contreras A., Angeles-Chávez C., Flores O., Perez R. Structural, morphological and interfacial characterization of Al—Mg/TiC composites. *Materials Characterization*. 2007;58:685—693. http://doi.org/10.1016/j.matchar.2006.11.031
24. Shu S., Lu J, Qiu F., Xuan Q., Jiang Q. Effects of alloy elements (Mg, Zn, Sn) on the microstructures and compression properties of high-volume-fraction TiC_x/Al composites. *Scripta Materialia*. 2010;63:1209—1211. http://doi.org/10.1016/j.scriptamat.2010.08.040
25. Gulyayev A.P. Metallovedeniye. Moscow: Metallurgiya, 1986. 544 p. (In Russ.).
Гуляев А.П. Металловедение. М.: Металлургия, 1986. 544 с.
26. Kolachev B.A., Elagin V.I., Livanov V.A. Metal science and heat treatment of non-ferrous metals and alloys. Moscow: MISIS, 2001. 433 p. (In Russ.).
Колачев Б.А., Елагин М.И., Ливанов В.А. Металловедение и термическая обработка цветных металлов и сплавов. М.: МИСИС, 2001. 433 с.
27. Arzamasov B.N., Sidorin I.I., Kosolapov G.F., Makarova V.I., Mukhin G.G., Ryzhov N.M., Silaeva V.I., Ulyanova N.V. Material science. Moscow: Mashinostroenie, 1986. 384 p. (In Russ.).
Арзамасов Б.Н., Сидорин И.И., Косолапов Г.Ф., Макарова В.И., Мухин Г.Г., Рыжов Н.М., Силаева В.И., Ульянова Н.В. Материаловедение. М.: Машиностроение, 1986. 384 с.
28. Lyakishev N.P. (Ed.). State diagrams of binary metallic systems: Reference book. In 3 volumes. Vol. 2. Moscow: Mashinostroenie, 1996. 498 p. (In Russ.).
Диаграммы состояния двойных металлических систем: Справочник. В 3 т. Т. 2. Под общ. ред. Н.П. Лякишева. М.: Машиностроение, 1996. 498 с.
29. Belov N.A. Phase composition of aluminum alloys. Moscow: MISIS, 2009. 234 p. (In Russ.).
Белов Н.А. Фазовый состав алюминиевых сплавов. М.: МИСИС, 2009. 234 с.
30. Kishchik M.S. Formation of a micrograin structure in aluminum alloy 1565ch by thermal and thermomechanical treatment: Abstract of the dissertation of Cand. Sci (Eng.). Moscow: MISIS, 2019. (In Russ.).
Кищик М.С. Формирование микрозеренной структуры в алюминиевом сплаве 1565ч путем термической и термомеханической обработки: Автореф. дис. ... к.т.н. М.: МИСИС, 2019.
31. Pan S., Wang T., Jin K., Cai X. Understanding and

designing metal matrix nanocomposites with high electrical conductivity: A review. *Journal Materials Science*. 2022;57:6487—6523.
http://doi.org/10.1007/s10853-022-07010-4

32. Pan S., Yuan J., Zheng T., She Z., Li X. Interfacial thermal conductance of in situ aluminummatrix nanocomposites. *Journals Materials Science*. 2021;56:13646—13658.
http://doi.org/10.1007/s10853-021-06176-7
33. Mikheev R.S., Chernyshova T.A. Discretely reinforced composite materials of the Al—TiC system (review). *Zagotovitelnye proizvodstva v mashinostroenii*. 2008; (11):44—53. (In Russ.).
Михеев Р.С., Чернышова Т.А. Дискретно армированные композиционные материалы системы Al—TiC (обзор). *Заготовительные производства в машиностроении*. 2008;11:44—53.
34. Rafalsky I.V. Resource-saving synthesis of aluminum-based alloys using dispersed non-metallic materials and intelligent methods for controlling metallurgical processes for their production. Minsk: BNTU, 2016. 309 p. (In Russ.).
Рафальский И.В. Ресурсосберегающий синтез сплавов на основе алюминия с использованием дисперсных неметаллических материалов и интеллектуальные методы контроля металлургических процессов их получения. Минск: БНТУ, 2016. 309 с.
35. Mikheev R.S. Promising coatings with improved tribotechnical characteristics from composite materials based on non-ferrous alloys. Abstract of the dissertation of Dr. Sci. (Eng.). Moscow: IMET RAS, 2018. (In Russ.).
Михеев Р.С. Перспективные покрытия с повышенными триботехническими характеристиками из композиционных материалов на основе цветных сплавов: Автореф. дис....д.т.н. М.: ИМЕТ РАН, 2018.
36. Perelygin Yu. P., Los I. S., Kireev Yu. S. Corrosion and protection of metals from corrosion. Penza: PGU, 2015. 88 p. URL: https://elib.pnzgu.ru/files/eb/u36mWX4yGz0I.pdf (accessed: 21.03.2023). (In Russ).
Перелыгин Ю. П., Лось И.С., Киреев С.Ю. Коррозия и защита металлов от коррозии. Пенза: Изд-во ПГУ, 2015. 88 с. URL: https://elib.pnzgu.ru/files/eb/u36mWX4yGz0I.pdf (дата обращения: 21.03.2023). (In Russ.).

Information about the authors

Alfiya R. Luts – Cand. Sci. (Eng.), Assistent Prof., Department of Metal Science, Powder Metallurgy, Nanomaterials (MPMN), Samara State Technical University (SamSTU).
http://orcid.org/0000-0001-7889-9931
E-mail: alya_luts@mail.ru

Yuliya V. Sherina – Post-graduate Student, Department of MPMN, SamSTU.
http://orcid.org/0000-0002-5451-7107
E-mail: yulya.makhonina.97@inbox.ru

Alexander P. Amosov – Dr. Sci. (Phys.-Math.), Head of the Department of MPMN, SamSTU.
http://orcid.org/0000-0003-1994-5672
E-mail: egundor@yandex.ru

Andrey D. Kachura – Master's Student, Department of MPMN, SamSTU.
http://orcid.org/0000-0001-9246-5638
E-mail: ruw223@mail.ru

Информация об авторах

Альфия Расимовна Луц – к.т.н., доцент кафедры металловедения, порошковой металлургии, наноматериалов (МПМН), Самарский государственный технический университет (СамГТУ).
http://orcid.org/0000-0001-7889-9931
E-mail: alya_luts@mail.ru

Юлия Владимировна Шерина – аспирант кафедры МПМН, СамГТУ.
http://orcid.org/0000-0002-5451-7107
E-mail: yulya.makhonina.97@inbox.ru

Александр Петрович Амосов – д.ф.-м.н., профессор, зав. кафедрой МПМН, СамГТУ.
http://orcid.org/0000-0003-1994-5672
E-mail: egundor@yandex.ru

Андрей Дмитриевич Качура – магистр кафедры МПМН, СамГТУ.
http://orcid.org/0000-0001-9246-5638
E-mail: ruw223@mail.ru

Contribution of the authors

A.R. Luts – concept, problem statement, analysis of the test results, paper authoring.

Yu.V. Sherina – heat treatment and testing of the samples, analysis of the test results, paper authoring.

A.P. Amosov – supervision, paper proofreading, conclusions editing.

A.D. Kachura – sample manufacturing, microstructural analysis, conclusions.

Вклад авторов

А.Р. Луц – формирование основной концепции, постановка цели и задачи исследования, анализ результатов, подготовка текста статьи.

Ю.В. Шерина – проведение термической обработки и испытаний образцов, анализ результатов, подготовка текста статьи.

А.П. Амосов – научное руководство, корректировка текста, корректировка выводов.

А.Д. Качура – синтез литых образцов, микроструктурный анализ, формулировка выводов.

The article was submitted 16.03.2023, revised 08.06.2023, accepted for publication 16.06.2023

Статья поступила в редакцию 16.03.2023, доработана 08.06.2023, подписана в печать 16.06.2023